Surface and Coatings Technology 174-175 (2003) 324-330

Effect of nitrogen gas flow on amorphous Si–C–N films produced by PVD techniques

C. Moura[a], L. Cunha[a,*], H. Órfão[a], K. Pischow[b], J. De Rijk[b], M. Rybinski[c], D. Mrzyk[c]

[a]*Physics Department, University of Minho, Campus de Gualtar, 4710-057 Braga, Portugal*
[b]*Savcor Coatings Oy, Insinöörinkatu 7, FIN-50100 Mikkeli, Finland*
[c]*Formerly at Physics Department, University of Minho, Campus de Gualtar, 4710-057 Braga, Portugal*

Abstract

$Si_xC_yN_z$ thin films were deposited by reactive magnetron sputtering on glass and steel substrates. The films were grown in a rotation mode over a carbon and a silicon targets in a mixed Ar/N_2 atmosphere at a substrate temperature of 300 °C. The substrates were held grounded or at a negative bias of −25 and −50 V. The film characteristics were also controlled by nitrogen flow. Binary and ternary films were obtained. The films were analysed with respect to microstructure, state of chemical bonding and optical properties by Raman spectroscopy (RS) and optical transmittance. RS was used as a probe of micro-structural modifications induced by deposition conditions. The main features observed in RS spectra are the well-known D- and G-bands characteristic of amorphous carbon. The position, widths and intensity ratio of these bands are found to be dependent on the film composition. The refractive index, the absorption coefficient and also the thickness were calculated from transmittance spectra obtained between 200 and 2500 nm. The hardness and Young's modulus of the films were measured by nano-indentation experiments. The average hardness and Young's modulus of the produced coatings was 21 and 200 GPa, respectively.

Keywords: Magnetron sputtering; Young's modulus; Nano-indentation experiments; Raman spectroscopy; Si-C-N films

1. Introduction

In many tribological applications wear resistance and corrosion protection are required. In addition, low surface energy is also important in order to avoid sticking effects.

Theoretical calculations predict that covalent bonded α- and β-C_3N_4 may present hardness and bulk modulus similar of diamond [1–4], but the synthesis of crystalline carbon nitride is difficult to achieve. In the case of carbon, low surface energy may be achieved by promoting sp^3-bonding states, reducing the amount of unsaturated bonds. Some attempts to obtain carbon nitride crystals have been made. The incorporation of some silicon in the growth of carbon nitride films by microwave plasma-enhanced CVD promoted the formation of crystallites [5], but the excessive Si incorporation led to the formation of amorphous phase in PVD process [6]. The growth of ZrN/CN_x super-lattices with carbon nitride (nitride to carbon ratio of 1.3) ultra thin layers (<2 nm) presented some crystalline regions [7] with sp^3 bond states.

Silicon nitride (Si_3N_4) is a well-known material and has high hardness, high fracture toughness, wear resistance, high thermal stability, chemical inertness and good insulating properties [8–10]. It is an interesting material for applications in which wear resistance is required at high temperature and in corrosive environments. Silicon nitride is also used for optical and electronic industry due to its dielectric properties, but these properties are strongly dependent on composition. The optical band-gap in SiN_x changes from 1.8 to 5 eV when x changes from 0 to 1.7.

Silicon carbide (SiC) is a hard ceramic, resistant to chemically aggressive environments, wear resistant and presents high thermal conductivity [8,11–13] and low thermal expansion. Silicon carbide is also an indirect semiconductor with wide energy band-gap (2.4–3.4 eV depending on polytype) [14].

The production of ternary system Si–C–N could exhibit interesting properties, in combining the charac-

*Corresponding author. Tel.: +351-253-604-066; fax: +351-253-678-981.
E-mail address: lcunha@fisica.uminho.pt (L. Cunha).

Table 1
Variable deposition parameters (N_2 flow or substrate bias), growth rate ($\dot{Z}$), density (ρ) and thickness (t_c) of $Si_xC_yN_z$ films

Samples prepared with variation of N_2 flow (Φ (N_2))					Samples prepared with variation of d.c. bias voltage (V_{Sub})				
Sample	Φ (N_2) (sccm)	$\dot{Z}$ (nm/min) (T/BC)	ρ (g/cm^3) (T/BC)	t_c (μm) (T/BC)	Sample	V_{Sub} (V)	$\dot{Z}$ (nm/min) (T/BC)	ρ (g/cm^3) (T/BC)	t_c (μm) (T/BC)
E3	0		–	0.4/–	–	–	–	–	–
F4	5	4.2/5.6	2.0/2.7	1.2/1.2	G3	0	3.5/6.0	1.7/2.9	1.2/1.5
F7	10	6.2/5.8	3.3/2.8	1.0/1.4	G12	−25	3.3/5.0	1.6/2.4	1.3/1.8
F2	20	4.2/5.4	2.0/2.6	1.8/1.7	F2	−50	4.2/5.4	2.0/2.6	1.8/1.7
G1	25	4.2/4.6	2.0/2.2	1.2/1.4	–	–	–	–	–

The *T* values were obtained for glass substrate samples using data obtained from transmittance spectra. The BC values were obtained for steel substrates samples, using data obtained from ball cratering measurements.

teristics of binary compounds—C_3N_4, Si_3N_4 and SiC. But Si–C–N systems have not been extensively studied. Most of the published work refers to high temperatures deposition processes like CVD techniques. These high temperatures (typically between 600 and 1200 °C) are a strong limitation for industrial applications. Only few experiments on synthesis of Si–C–N have been carried at low growth temperatures. Pulsed laser deposition was used by some authors [15,16], but also ion sputtered deposition of carbon and silicon in a nitrogen atmosphere, with simultaneous nitrogen ion bombardment of substrates [17], reactive magnetron sputtering [18–20].

In the present work it is reported the deposition and characterization Si–C–N coatings on glass and steel substrates. The effect of nitrogen flow (0–25 sccm) and substrate bias (grounded, −25 and −50 V) was studied, using non-destructive Raman spectroscopy (RS) and optical transmittance. In fact, an understanding of the local chemical bonding is necessary to optimise the growth parameters for improvement of the physical properties. However, the investigation of the structural arrangements is not straightforward since five types of bonds (Si–Si; Si–C; C–C; Si–N; C–N) are present in this disordered material. Moreover, the ability of carbon to present sp^2 or sp^3 coordination adds some complexity to the bonding states.

2. Sample preparation and experimental techniques

The samples were deposited by reactive r.f. magnetron sputtering, in a rotation mode (4 rpm) from high purity C and Si targets, onto polished stainless steel (AISI 316) and glass substrates. The option for these two kinds of substrates was mainly related to the kind of physical properties to be measured. The depositions were carried out in an Ar/N_2 atmosphere using an Alcatel SCM650 apparatus. Prior to all depositions, the substrates were ultrasonically cleaned and sputter etched for 10 min in a 0.4 Pa argon atmosphere (200 W r.f. power). During deposition experiments the substrate temperature was 300 °C, the target–substrate distance was 65 mm and argon flow was 100 sccm. Two series of samples were produced: the first set was prepared with constant substrate d.c. bias (−50 V) and r.f. power applied to the magnetrons (P_C = 500 W and P_{Si} = 100 W), but five different values of nitrogen flow were used, (0–25 sccm); the second set was prepared with constant nitrogen flow (20 ccm) and r.f. power applied to the magnetrons (P_C = 500 W and P_{Si} = 100 W), but three different substrate d.c. bias were applied (grounded, −25 and −50 V). The reason for the difference of power applied to carbon and silicon targets is related with their different size. The power per unit area is 1.6 and 2.3 W/cm^2 for carbon and silicon targets, respectively. The total pressure during experiments was approximately 0.5 Pa. The summary of the deposition parameters is shown in Table 1.

The thickness of the coatings deposited on steel substrates was measured by ball cratering (thickness BC in Table 1). The hardness and Young's modulus were measured perpendicularly to the surface with a microprobe equipped with a Berkovich diamond indenter (Nanoindenter XP), using the method of Oliver and Pharr [21]. The load measurement resolution was 1 μN. The instrumented indentation depths were 100 nm and they were achieved with average loads between 2.695 and 4.110 mN. The nano-hardness and Young's modulus values were achieved by calculating the average of the results obtained by 20 indentations in each film.

The transmittance spectra were obtained in a Shimadzu UV-3101PC spectrophotometer, with wavelength range between 200 and 2500 nm. The spectra were obtained in 2 nm steps and the slit width was 2 nm. These spectra were used to obtain the thickness of the samples deposited on glass (thickness *T* in Table 1), but also the refraction index and absorption coefficient using Swanepoel method [22].

The density of the coatings was estimated from mass gain of the samples during deposition divided by the volume of the film. This volume was calculated as the product of deposited area by film thickness. Table 1 shows two density values for each film (*T* and BC): the density T is estimated by using the film thickness obtained by transmittance spectra (glass substrates); the density BC is estimated by using film thickness measured by ball cratering (steel substrates).

The Raman scattering analysis of different films has been performed at room temperature using the 488 nm line of an argon ion laser. The measurements were performed with a BHSM Olympus microscope using ×100 MS Plan objective. To limit local heating of the sample the power of incident light onto the sample was 2.5 mW. The scattered light was detected by a triple monochromator Jobin Yvon T64000 coupled to a CCD detector. The spectra have been recorded over a very wide frequency range (200–2500 cm^{-1}).

The structure analyses were made after X-ray diffraction (XRD), using Cu Kα radiation in a θ–2θ set-up.

This study will show the variation of some physical properties and microstructure of the films with the nitrogen flow during deposition, but also with substrate bias. Future studies will show other dependencies.

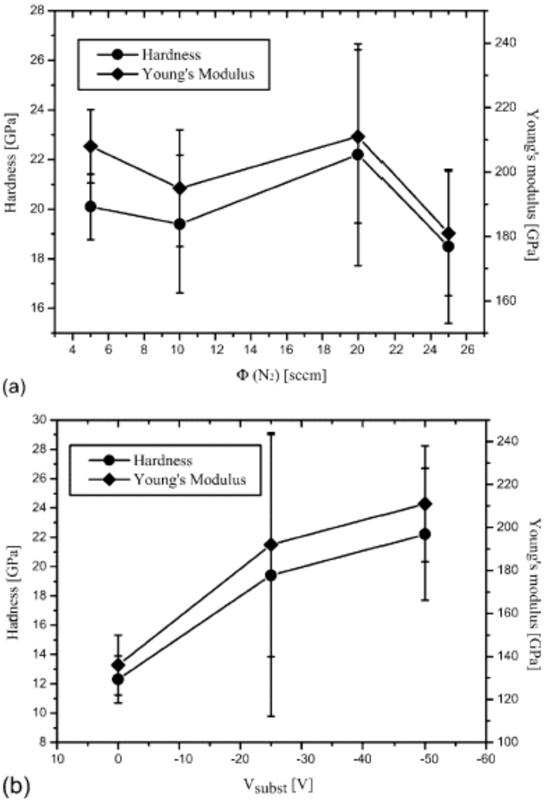

Fig. 1. Hardness and Young's modulus of $Si_xC_yN_z$ films measured by nano-indentation and prepared at: (a) constant bias voltage (−50 V) and different nitrogen flow; (b) constant nitrogen flow (20 sccm) and different bias voltage.

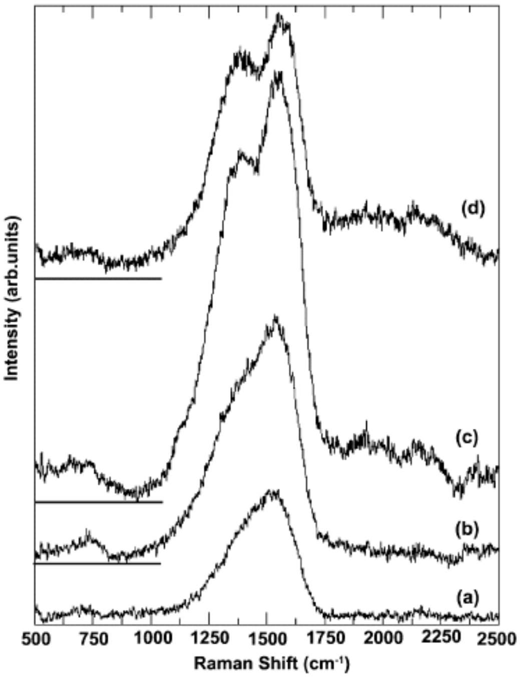

Fig. 2. Raman scattering spectra of $Si_xC_yN_z$ films prepared with different nitrogen flow: (a) $\Phi(N_2)=5$ sccm; (b) $\Phi(N_2)=10$ sccm; (c) $\Phi(N_2)=20$ sccm; (d) $\Phi(N_2)=25$ sccm.

3. Results and discussion

3.1. Dependence on the nitrogen flow

The density of the films deposited on steel substrates is higher for lower values of the nitrogen flow. The decrease of the density of the films, when the nitrogen flow increases may be explained by higher porosity due to higher pressure during deposition. In general the coatings deposited on steel substrates are denser because of the ion bombardment during deposition, caused by the negative d.c. bias.

The dependence of hardness and Young's modulus on nitrogen flow cannot be deduced (Fig. 1). The average hardness and Young's modulus of the coatings are approximately 21 and 200 GPa, respectively. It is interesting to verify that in general, the standard deviation of nano-indentation experiments increases with the increase of nitrogen flow during experiments. This is an indirect observation of the increase of the porosity of the films when the nitrogen flow is higher. This result is in accordance with the general decrease of density of the films when the N_2 flow increases and with the predictions of Thornton model.

RS was used as a probe to verify the changes in the films microstructure. The Stokes part of the Raman

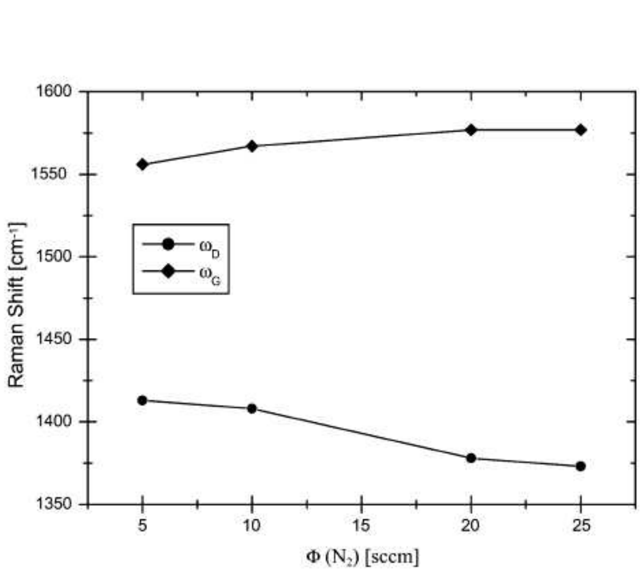

Fig. 3. Dependence of G-band (ω_G) and D-band (ω_D) Raman frequency as function of nitrogen flow.

spectra between 500 and 2500 cm^{-1} obtained for the samples deposited with different nitrogen flow are shown in Fig. 2. They are composed of broad features characteristic of the amorphous nature of the film, confirmed by XRD, and dominated by intense and asymmetric bands in the region between 900 and 1900 cm^{-1}. They are the well-known G-band centred approximately 1540 cm^{-1} and D-band centred approximately 1400 cm^{-1} associated with disordered-allowed zone edge modes of disordered graphitic carbon, that become Raman active due to the lack of long-range order [23]. In all spectra registered in Fig. 2, less intense structures are detected. In the low frequency range, the band located approximately 750 cm^{-1} is attributed to optical-like modes of hetero-polar Si–C bonds. In the high frequency range the band located approximately 2200 cm^{-1} is ascribed to C≡N vibrations.

To study the influence of the nitrogen flow in the bonding state of the deposited films, it is crucial to know the correct position of the D and G bands, since the ratio of the intensities of these D and G bands, I_D/I_G, has been shown to correlate inversely with both the

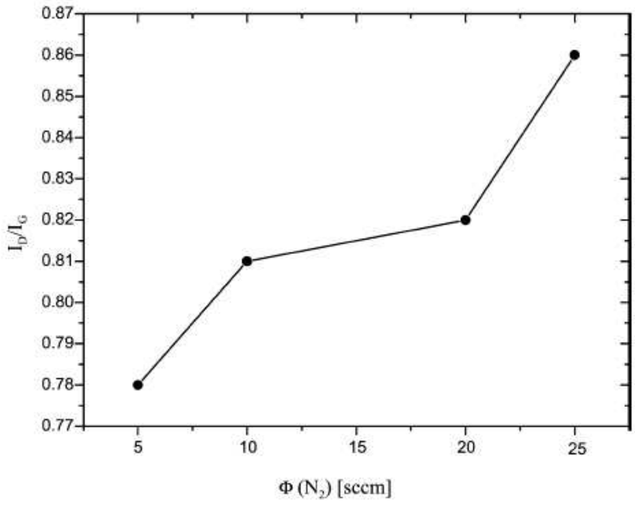

Fig. 4. I_D/I_G ratio as function of nitrogen flow (I_D—intensity of D-band; I_G—intensity of G-band).

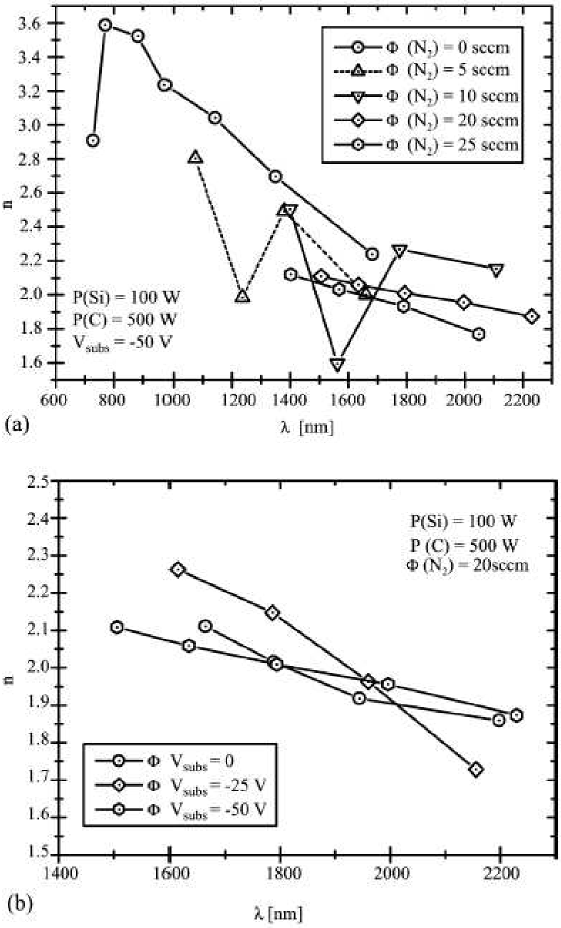

Fig. 5. Refraction index of $Si_xC_yN_z$ films calculated from transmittance spectra and prepared at: (a) constant bias voltage (−50 V) and different nitrogen flow; (b) constant nitrogen flow (20 sccm) and different bias voltage.

size and the density of graphite crystallites [24–26]. In order to improve the frequency position of the bands, the obtained Raman spectra were fitted by using two Gaussian functions. The frequency dependence of G and D-bands is shown in Fig. 3. The dependence of intensity ratio of G to D peak on nitrogen flow is shown in Fig. 4. The ratio I_D/I_G and the position of G-band (ω_G) increases while the position of D-band (ω_D) decreases, with nitrogen content. Usually this ratio is correlated with the decrease in sp^3 carbon fraction, induced by grain boundaries or substitution of sp^3 carbon atoms by N atoms. This is consistent with an increase in the size or number of graphitic domains in the film [27].

The results obtained from transmittance spectra show that generally the refractive index of the films, obtained between 200 and 2500 nm, decreases with increase of N_2 flow during deposition. The films produced without N_2 flow have the highest refractive index (Fig. 5). The absorption coefficient of the Si–C–N coatings is not significantly different, excepting the film produced without nitrogen flow. The higher values were detected for the coating produced with a N_2 flow of 10 sccm. Although, the sample produced without nitrogen during the deposition, has a significantly lower absorption coefficient (Fig. 6).

3.2. Dependence on the applied bias voltage

The density of the films deposited on steel substrate is higher (between 2.4 and 2.9 g/cm^3) than those deposited on glass substrates (between 1.6 and 2.0 g/cm^3).

As expected, the coating produced with higher sub-

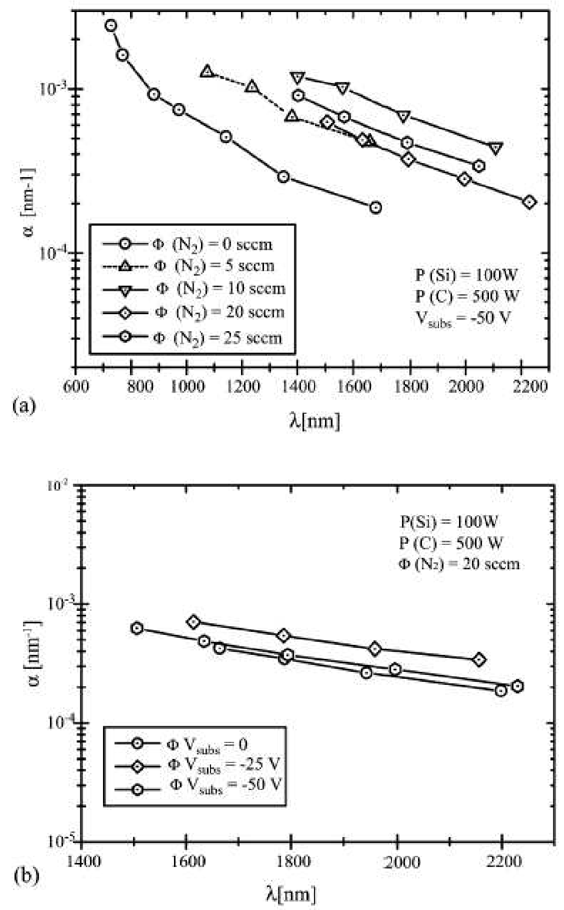

Fig. 6. Absorption coefficient of $Si_xC_yN_z$ films calculated from transmittance spectra and prepared at: (a) constant bias voltage (−50 V) and different nitrogen flow; (b) constant nitrogen flow (20 sccm) and different bias voltage.

Table 2
Experimental results obtained from Raman spectra of $Si_xC_yN_z$ films deposited with variation of substrate bias: I_D—intensity of D-band; I_G—intensity of G-band

Bias (V)	Raman peak position (cm^{-1})		I_D/I_G
	ω_D	ω_G	
0	1392	1573	0.78
−25	1406	1567	0.80
−50	1378	1577	0.82

strate bias presents higher nano-hardness (22.2 GPa) and Young's modulus (201 GPa) (Fig. 1). This is due to the higher compactness of the film, in consequence of higher ion bombardment during deposition.

Raman spectra of films deposited with different substrate bias were also obtained and they are very similar to those shown in Fig. 2. In Table 2 is listed the experimental data obtained from the Raman spectra. The peak position of G band does not have significant changes, but the intensity ratio of D to G bands increases with the increase of the negative bias and the D band shifts to lower frequencies. These results suggest an increase of the size of the sp^2-bonded micro-domains due to the negative bias. In fact, an increase of the bias will probably rise the substrate temperature and some rearrangements occur in the samples resulting in an ordered structure of the films [25,26]. Raman spectra and XRD patterns confirm the amorphous nature of the coatings.

The refraction index and absorption coefficient of the samples deposited with variation of the substrate bias are similar (Figs. 5 and 6). Although, the refraction index of the sample with −25 V bias decreases faster than the other two samples. This same sample has a slightly higher absorption coefficient compared to grounded and −50 V bias produced samples.

4. Conclusion

The analyses of the $Si_xC_yN_z$ thin films produced by r.f. reactive magnetron sputtering showed the following results:

Two main bands at 1400 and 1540 cm^{-1} can be distinguished from the Raman spectra of the films, which indicate the amorphous nature of the deposited coatings. These results were confirmed by XRD.

The intensity ratio of I_D/I_G, in Raman spectra, increases with nitrogen content due to the decrease in sp^3 carbon fraction. A similar behaviour is obtained when the ion bombardment increases during deposition. This may indicate a tendency to a less disordered nature of the films.

The refraction index is between 1.6 and 2.8, but the variation of this optical property with the wavelength of the incident radiation, is similar for the coatings produced with higher nitrogen flow during deposition (20 and 25 sccm). For these two samples the curve has the same behaviour and this optical property varies between 1.8 and 2.2 when the wavelength varies between 1400 and 2200 nm. The behaviour of the refraction index curve for samples produced with the same nitrogen flow (20 sccm), but different bias, is similar. The order of magnitude of the absorption coefficient for all the samples produced with nitrogen flow during deposition is 10^{-3} nm^{-1}.

The increase of ion bombardment during deposition increases the hardness and Young's modulus of the produced films.

Acknowledgments

The authors gratefully acknowledge Mr Massoun Atfeh, from Savcor Coatings Oy (Finland) for the help in obtaining XRD data and nano-indentation measurements.

References

[1] S. Boughaba, G.I. Sproule, J.P. McCaffrey, M. Islam, M.J. Graham, Thin Solid Films 402 (2002) 99.
[2] A.Y. Liu, M.L. Cohen, Science 245 (1989) 841.
[3] A.Y. Liu, M.L. Cohen, Phys. Rev. B 41 (1990) 10727.
[4] C.-M. Sung, M. Sung, Mater. Chem. Phys. 43 (1996) 1.
[5] L.C. Chen, C.K. Chen, D.M. Bhusarim et al., Materials Research Society Symposium Proceedings 468 (1997) 31.
[6] L.C. Chen, C.T. Wu, J.-J. Wu, K.H. Chen, Int. J. Mod. Phys. B 14 (2–3) (2000) 333.
[7] M.L. Wu, M.U. Guruz, V.P. Dravid, et al., Aool. Phys. Lett. 76 (2000) 2692.
[8] N.S. Jacobson, E.J. Opila, D.S. Fox, J.L. Smialek, Mater. Sci. Forum 251–254 (1997) 817.
[9] F.-L. Riley, J. Am. Ceram. Soc. 83 (2000) 245.
[10] M.J. Hoffman, Mater. Res. Soc. Bull. 20 (1995) 28.
[11] S.S. Shinozaki, Mater. Res. Soc. Bull. 20 (1995) 42.
[12] V.D. Krstic, Mater. Res. Soc. Bull. 20 (1995) 46.
[13] H. Matsunami, in: K.J. Klabunde (Ed.), Thin Film from Free Atoms and Particles, Academic Press, Orlando, FL, 1985, p. 301.
[14] W.J. Choyke, G. Pensl, Mater. Res. Soc. Bull. 22 (1997) 25.
[15] T. Thärigen, G. Lippold, V. Riede, et al., Thin Solid Films 348 (1999) 103.
[16] R. Machorro, E.C. Samano, G. Soto, L. Cota, Appl. Surf. Sci. 127–129 (1998) 564.
[17] Z. He, G. Carter, J.S. Collignon, Thin Solid Films 283 (1996) 90.
[18] S. Komatsu, Y. Hirohata, S. Fukuda, et al., Thin Solid Films 193–194 (1990) 917.
[19] L.C. Chen, H.Y. Lin, C.S. Wong, et al., Diamond Relat. Mater. 8 (1999) 618.
[20] T. Berlind, N. Hellgren, M.P. Johansson, L. Hultman, Surf. Coat. Technol. 141 (2001) 145.

[21] W.C. Oliver, G.M. Pharr, J. Mater. Res. 7 (1992) 1564.
[22] R. Swanepoel, J. Phys. L. Sci. Instrum. 18 (1983) 1214.
[23] A. Chehaidar, R. Carles, A. Zwick, C. Meunier, B. Cros, J. Durand, J. Non-Cryst. Solids 169 (1994) 37.
[24] R. Schlesinge, M. Bruns, H.J. Ache, J. Electrochem. Soc. 144 (1997) 1.
[25] M.M. Lacerda, F.L. Freire Jr., G. Mariotto, Diamond Relat. Mater. 7 (1998) 412.
[26] Y.H. Cheng, X.L. Qiao, J.G. Chen, et al., Diamond Relat. Mater. 11 (2002) 1511.
[27] M.M. Lacerda, D.F. Franceschini, F.L. Freire Jr., G. Mariotto, Diamond Relat. Mater. 6 (1997) 631.